UCRL- 90319
PREPRINT

Unsteady Heat Transfer During Laminar Flame Quenching

S. R. Vosen

R. Greif

C. K. Westbrook

This paper was prepared for submittal to the
20th International Symposium on Combustion,
Ann Arbor, Michigan, August 12-17, 1984

January 23, 1984

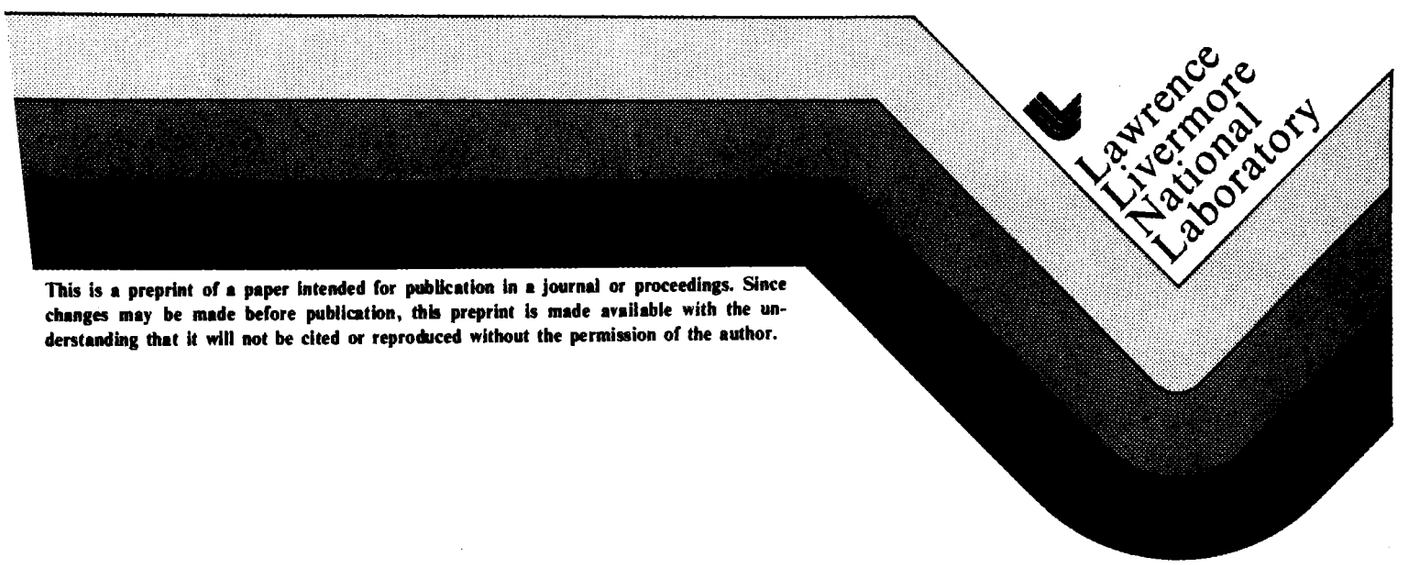

DISCLAIMER

UNSTEADY HEAT TRANSFER DURING LAMINAR FLAME QUENCHING

by

S. R. Vosen *, R. Greif

Mechanical Engineering Department and
Applied Science Division, Lawrence Berkeley Laboratory
University of California,
Berkeley, CA 97420

and

C. Westbrook

Lawrence Livermore National Laboratory,
Livermore, CA 94550

ABSTRACT

Measurements were made of the unsteady heat transfer to a wall during the quenching of premixed, methane-air flames. One dimensional laminar flames were produced in a constant volume chamber and the heat transfer into the quenching surface was measured by means of a platinum thin film resistance thermometer. The experiments were performed at pressures near atmospheric over a range of equivalence ratios from 0.7 to 1.2. Predictions of the heat transfer were made with two numerical finite difference models, one with detailed kinetics and the other with single step kinetics.

The main experimental results are: 1) the data are successfully correlated using the heat release rate of the flame prior to quenching; 2) the maximum heat flux is related to the quenching distance and thus it may be possible to use measurements of the quenching distance to predict the maximum heat flux.

Present Address:
* Combustion Research Facility, Sandia National Laboratory, Livermore, CA 94550

A comparison of the experimental results and the numerical calculations revealed that: 1) A single step reaction model predicts the heat transfer as well as a detailed kinetics model, to within 15% of the experimental results; 2) thermal diffusion and the chemical reaction rate of combustion are the dominant processes which determine the heat flux during quenching.

1 INTRODUCTION

The unsteady heat transfer to the walls of a combustion chamber depends upon many factors, many of which are not well understood. In practical devices, such as internal combustion engines, several complicated and closely coupled processes occur simultaneously. For example, the flow is turbulent, boundary conditions are unsteady, the quality of the fuel can vary, and radiation can be significant. In an attempt to obtain a basic understanding of these phenomena, many of them have been studied separately[1,2]. The purpose of this work was to obtain measurements and develop models to predict the unsteady heat transfer during flame-wall interactions (flame quenching). Specifically, the unsteady interaction of laminar, premixed, methane-air flames in stagnating flows were studied as they approached a cold wall. Thin film resistance thermometers were used to determine the unsteady heat flux.

The heat transfer during flame quenching has been determined in many different systems, such as: detonation tubes[3]; shock tubes[4,5]; constant volume combustion chambers[6,7]; and internal combustion engines[8,9]. Modeling of the heat transfer is difficult for most of these cases, and as the complexity of the system increases, the models become increasingly empirical. It is shown in this study that the heat transfer in a constant volume chamber may be predicted by solving the basic conservation equations with experimentally determined kinetics parameters.

A review of heat transfer studies in systems with combustion may be found in ref.

10.

2 EXPERIMENTAL SYSTEM

The experiments were performed in a constant volume combustion chamber (Fig. 1). The chamber was designed specifically for these experiments, with the flexibility for use as a general purpose, low pressure container with good accessibility to its interior.

The combustion chamber were constructed from 5/8" thick, type 303 stainless steel seamless tubing The interior of the container has the shape of two 3.50 inch diameter cylinders 7 inches long, intersecting at right angles. Along the third axis, instrumentation ports were provided on the top and bottom of the container. Two additional ports on the off optical axis provide for the introduction of fresh reactants, and the exhausting of burnt gases.

The oxidizer (air) and fuel (99.98% pure methane) are obtained from high pressure bottles, and individually flow through rotameters before being mixed at approximately 8 psi.

The gas flow rates while the chamber was being charged was monitored by rotameters (Matheson), and were adjusted by needle valves. The rotameters were calibrated by the soap bubble method. This method of calibration gave an uncertainty in the equivalence ratio of approximately 2%.

Ignition of the unburnt gases was accomplished by means of an 8 kilovolt, 200 millijoule discharge across a .035 inch gap between 0.020 inch tungsten electrodes. The electrodes are mounted in the chamber through one of the 4 inch ports that are off of the optical axis. A plexiglass insert with compression fittings provides a convenient way of adjusting the electrode gap and position in the chamber.

Three measurements are made during an experimental run: the chamber pressure, the wall heat flux at one location, and schlieren or shadowgraph photography. A schematic of the experimental setup is shown is Fig. 2.

The pressure in the chamber was measured at the bottom instrumentation port. The output of the pressure transducer, which was of the piezioelectric type (AVL model 12QP300cvk), was passed through a charge amplifier (Kistler model 566) and was recorded on an oscilloscope.

The wall heat flux was determined from measurements made with thin film resistance thermometers on a ceramic base. The gauge was mounted flush in a metal fixture, which was in turn mounted in the chamber. Leads from the thin film pass through the ceramic base to a bridge amplifier, and the output was recorded on an oscilloscope.

The thermal properties of the substratum are known from the manufacturer (Corning Glass Works). Thus the primary step in the calibration procedure was the determination of the output of the thin film and associated electronics as a function of the temperature of the thin film.

The temperature sensor - amplifier combination was calibrated quasi-steadily in an oven. A thermocouple embedded in the ceramic gave an absolute measure of the temperature, which was then compared to the bridge amplifier output. The calibration determined in this manner was linear to within three percent over the temperature range encountered in the experiments (25 to 75 C).

Optical measurements were obtained from either schlieren or shadowgraph photography, made by use of the standard Z configuration schlieren. The light source was a delayed microsecond spark light for stills, and a continuous source for use with a 5000 frame per second movie camera (Hycam model 41-0004). An aperture and razor edge were both tried for the schlieren pictures. Due to the three dimensional structure of the flame, the aperture worked best for an overall view of the flame.

As discussed above, the output of the thin film gauge and the pressure transducer were recorded on an oscilloscope. The oscilloscope traces were then digitized using a model 4662 Tektronics plotter driven by a PDP 11/34 computer. The appropriate cali-

bration constants were then applied and linear interpolation was used between data points which were evenly spaced in time. The wall heat flux was then determined from the Duhammel Integral resulting from the unsteady heat transfer problem in the solid[5.11]. The data from 3 - 10 runs were averaged to give the results presented in section 3. In all cases the run to run variation in the data produced an error in the heat flux that was only 5% of the value of the maximum heat flux.

3 EXPERIMENTAL RESULTS

The experimental results from this study are the unsteady wall heat fluxes during the quenching of a planar, laminar methane-air flame. Data were obtained at pressures near atmospheric for equivalence ratios varying from φ = 0.70 to φ = 1.20 (cf. Table I).

The experimental data were nondimensionalized (Fig. 3) based on the properties of a flame propagating into a gas at a pressure of p_q and an unburnt gas temperature of T_u, (defined in section 4) that is, for the conditions of the bulk unburnt gas at the time that quenching occurs. For methane-air flames, the Lewis number is near one, and the time and heat flux can be scaled by the thermal properties of a freely propagating flame. The characteristic time is given by the flame speed and thermal diffusivity according to:

$$t_c = \left(\frac{\alpha}{S_u^{\,2}} \right)_{p_q, T_u} \quad . \tag{1}$$

The characteristic heat flux is given by the heat release rate in an undisturbed flame:

$$q_c = (\rho S_u c_p \Delta T_f)_{p_q, T_u} \quad . \tag{2}$$

S_u is the laminar flame speed, ρ the density, and c_p the specific heat of the gas. The values of t_c and q_c for methane-air, calculated from Eqs. (1) and (2), are given in Table I. Values of the thermal properties are taken from ref. 12 and the flame properties from ref 13.

The dimensionless heat flux variation is presented in Fig. 3. It is seen that the data are successfully correlated using t_c and q_c over the range $0.70 \leq \varphi \leq 1.20$. In particular, note the large variation of the dimensional maximum value of the heat flux $q_{w\,max}$ (Table I) in contrast to the small variation in $q_{w\,max}/\,q_c$. The maximum heat flux is attained at an equivalence ratio of 1.1, which is consistent with the maximum value of the heat release q_c.

Unlike experiments involving more complex geometries[7], all of the results in the constant volume cell show similar trends. The wall heat flux increases slowly until the flame reaches the vicinity of the wall where the heat flux gauge was located. The wall heat flux then increases rapidly to a maximum value, after which the flux falls as the inverse square root of the time. In order to characterize the shape of the curves, the interval of time, t_q, required for the heat flux to increase from 50% of the maximum heat flux to the maximum heat flux will be used. These time intervals and the values of the maximum heat flux for all of the conditions are listed in Table I.

INTERPRETATION OF RESULTS

It is helpful to utilize some results from the numerical calculations (which are presented below) to aid in the interpretation of the experimental results. In Fig. 4, some pertinent information is presented. The top curve shows the distance from the flame to the wall as a function of time. The two curves on the bottom half of the figure show the variation of the total chemical heat release and the wall heat flux on the same time scale.

Initially, the flame speed and heat release in the flame are not affected by the wall, even though the wall heat flux (which is small) rises at an increasing rate. As the wall heat flux increases, the effect of the wall on the flame propagation also increases. Eventually, the flame begins to decelerate, and the heat release in the flame starts to drop. During this time, the wall heat flux is increasing almost linearly with time.

The flame ultimately reaches a position where the heat losses are so great that it can no longer move further. The flame then remains stationary while fuel near the wall diffuses towards the flame. The wall heat flux reaches a maximum value and then decreases as the last of the fuel is consumed. This interpretation is supported by both the experimental results of Fig. 3, and the photographic evidence, ref. 10.

4 NUMERICAL RESULTS

Two models of the quenching process were used to predict the unsteady heat transfer. These were both finite difference models[14], one with detailed kinetics[15], and the other with global, single step kinetics[16]. In each of the models, the conservation equations governing reactive-diffusive gas mixtures were used, with the assumptions that species diffusion was dominated by concentration gradients, and that radiative heat transfer is not important.

The conditions in the experiment were modeled by considering the interaction of a steady laminar flame with an impervious wall of very large heat capacity. The rate of increase of the pressure in the experiment was small, and so the pressure was taken to be constant. This was accomplished by considering the gas to be of semi-infinite extent, bounded only by the wall at which quenching occurs.

In the calculations, the constant value of the pressure was chosen to be the value at the time of quenching, p_q. The unburnt gas far in front of the flame is taken to be adiabatically compressed from the inital conditions ($T = T_o$, $P = P_o$) to the temperature $T_u = T_o(p_q / p_o)^{\gamma-1/\gamma}$, where γ the ratio of specific heats (c_p / c_v). The wall temperature is also taken to be equal to the value T_u. In general, the wall temperature is a function of the thermal properties of the wall and the wall heat flux. For experiments in constant volume combustion chambers, the wall temperature before quenching will be between the initial wall temperature, T_o, and T_u. Thus a thermal boundary layer will exist at the wall. For pressures near the initial pressure, such as those under con-

sideration, the boundary layer is weak and does not significantly affect the heat transfer. However, at higher pressures, the effect of the thermal boundary layer on the heat flux can be appreciable[10].

DETAILED KINETICS VS. SINGLE STEP KINETICS MODELS

Calculations were performed for methane-air flame quenching using two models for the kinetics. One utilized 86 chemical reactions and is denoted as the detailed kinetics model[15]. The other model used a single step, global reaction, where the reaction rate constants were chosed to produce good agreement with experimental values of the flame speed and flame temperature[16]. The two predictions for the heat flux differed by less than 10% of the maximum heat flux. Because the single step model requires much less computer time than the detailed model, (and gives good agreement with the detailed model), single step kinetics was chosen for all of the subsequent calculations.

Using the single step kinetics model, the effect of equivalence ratio on the heat transfer was studied. These results are summarized in Table I and in Fig. 5. It is seen that the results for all equivalence ratios are brought together by using the parameters of section 3. These results are similar to the results of Kurkov[17], who also used a single step reaction.

5 COMPARISON OF EXPERIMENTAL AND NUMERICAL RESULTS

The ranges of both the experimental data for the heat flux (Fig. 3) and numerical results (Fig. 5) are shown in Fig. 6. The agreement between the results is good, with the single step kinetics model predicting the heat flux over the equivalence ratio range from 0.70 to 1.20. The kinetics parameters in the single step model were determined by requiring the model to reproduce experimental values of the flame speed and temperature. From the agreement between the experiment and model, we may infer that these are also important quantities in determining the heat transfer during the

unsteady quenching of the flame.

COMPARISON WITH OTHER EXPERIMENTS

Unsteady heat transfer measurements during flame quenching have been made under a variety of conditions (cf. Introduction). Measurements of the steady state heat transfer from one dimensional porous burner butane flames have been made by Yamazaki & Ikai[18], who successfully modeled the heat transfer using a thermal model of flame propagation. Their results for the heat transfer rate, q_w / q_c, are from 5 to 10 times less than the values which were measured in the present study. It is noted that the porous burner has wall blowing which reduces the heat transfer to values less than the impermeable wall results.

The study of Isshiki and Nishiwaki[6] is pertinent to the present work. They carried out unsteady heat transfer measurements with H_2-O_2 flames. In addition, they utilized a simplified thermal model of flame propagation to obtain the following result for the maximum heat flux:

$$q_{w\,max} = \frac{2k_o \Delta T_f}{(\pi \alpha_o t_f)^{1/2}} \left[\frac{p_q}{p_o}\right]^{1/2} , \qquad (3)$$

where t_f *is the total time required* for *quenching* as determined from wall temperature measurements†. The value for t_f was obtained from measurements of the (variable) wall temperature. The agreement between their experimental values of the maximum heat flux and the maximum value from Eq. (3) was quite good.

In order to simplify the comparison of the work of Isshiki & Nishiwaki with the present study, the characteristic heat flux (q_c) and the characteristic time (t_c) are substituted into Eq. (3), along with the experimentally determined relationship $t_f \approx 2t_q$, to give:

$$\frac{q_{w\,max}}{q_c}\left[\frac{t_q}{t_c}\right]^{1/2} = \left[\frac{2}{\pi}\right]^{1/2}\left[\frac{k_o \rho_o c_{p\,o} p_q}{k_w \rho_w c_{p\,w} p_o}\right]^{1/2} ,$$

† The time t_f is not to be confused with t_q, defined in section 3, which is the time required for the heat flux to rise from 50% to 100% of its maximum value. From the present experimental data, $t_f \approx 2t_q$ (Fig. 4).

The wall temperature, T_w, is approximately equal to the initial temperature, T_o, so $k_o = k_w$, $c_{po} = c_{pw}$, and $\rho_o = (p_o / p_q)\rho_w$. Thus the above equation reduces to

$$\frac{q_{w\,max}}{q_c}\left(\frac{t_q}{t_c}\right)^{1/2} = \left(\frac{2}{\pi}\right)^{1/2} \approx 0.80 \qquad (4)$$

For the present experiments, we have that (cf. Table I):

$$\frac{q_{w\,max}}{q_c}\left(\frac{t_q}{t_c}\right)^{1/2} = 0.57 \pm 10\% \qquad (5)$$

The agreement between the results of this experiment (Eq. (5)) and the results of Isshiki & Nishiwaki (Eq. (4)) is quite good. Isshiki & Nishiwaki showed that Eq. (4) successfully correlated the maximum heat flux. The results of this work have been shown to reduce to the result of Isshiki & Nishiwaki (Eq. (5)), and more importantly also provide a basis for correlating the quenching time and the heat flux independently. Specifically, from Table I, $q_{w\,max} / q_c \approx const \approx 0.4$, and $t_q / t_c \approx const \approx 2.0$.

THE RELATIONSHIP OF THE HEAT FLUX TO THE QUENCHING DISTANCE

The maximum wall heat flux during quenching is related to the closest approach of the flame to the wall, and thus correlations of this quenching distance may be useful in predicting the maximum heat flux. A length scale for quenching may be defined as:

$$\delta_T \equiv \frac{\Delta T_f\, k_w}{q_{w\,max}} \quad , \qquad (6)$$

where ΔT_f is the the temperature difference across the flame, and k_w is the thermal conductivity of the fuel air mixture at the wall. The length δ_T is related to the temperature profile in the gas during quenching, and thus is also related to the quenching distance as measured by other techniques.

From both experimental and theoretical quenching studies, it has been shown that the Peclet number for the quenching distance††, is a constant, or at most a function of the gas kinetics[15,17,19,20]. The Peclet number for quenching, based on the pro-

†† The Peclet number is given by $Pe = LS/\alpha$, where L is a length scale, S is the fluid speed, and α is the thermal diffusivity of the gas.

perties of the unburnt gas is:

$$Pe_u = \rho_u S_u \frac{c_{pu}}{k_u} \delta_T = \frac{q_c}{q_{w\,max}} \frac{k_w}{k_u} \quad . \tag{7}$$

From the experimental results for $q_{w\,max}/\,q_c$ (cf. Table I), and $k_u/\,k_w \approx (T_u/\,T_w)^{0.681}$ (ref. 10) we have†††

$$Pe_u = 2.4 \pm 10\% \quad . \tag{8}$$

Another result for the Peclet number may be obtained from the numerical result for $q_{w\,max}/\,q_c$ using single step kinetics (cf. Table I). Recall that the calculations used $T_w = T_u$, so that $k_w = k_u$. Thus we obtain:

$$Pe_u = 2.5 \pm 12\% \quad . \tag{9}$$

The nondimensional maximum heat flux during unsteady flame quenching has been shown to be related to the Peclet number for quenching (Eq. (7)). Therefore we have that the experimental results and the numerical results both predict the same value for the Peclet number. This is consistant with the results of quenching distance studies, which predict small variations in the Peclet number[19].

6 CONCLUSIONS AND RECOMMENDATIONS

EXPERIMENTAL RESULTS

Measurements have been made of the heat transfer to a wall during the quenching of a premixed, methane-air flame. The geometry of the interaction of the flame with the wall was essentially one dimensional, and the flame was laminar prior to quenching. The experiments were performed at nearly atmospheric pressure over a range of equivalence ratios from 0.7 to 1.2.

1) The data were successfully correlated using the heat release rate in a steady, laminar flame. This incorporated the effects of the equivalence ratio.

---

††† In the experiments, $k_u/\,k_w$ was nearly constant, varying from 1.03 to 1.05.

2) There is a very strong connection between the experimental maximum heat flux and the experimental values of the quenching distance. It may be possible to use these results in conjunction with measurements of the quenching distance for other fuels to infer the corresponding heat fluxes.

EXPERIMENTAL AND NUMERICAL RESULTS

For the range of experimental conditions covered, a comparison of the experimental results and the numerical calculations yields the following:

1) A one dimensional finite difference model with single step Arrhenius kinetics predicts the heat transfer to an accuracy of ±15%.

2) A comparison of the results of the numerical models with the experimental results indicates that the thermal diffusivity ,the flame speed, and the flame temperature are of primary importance in determining the heat flux during quenching.

3) The reaction rate parameters in the single step model may be determined by matching the numerical and experimental values of the flame speed and temperature. Thus the model may prove useful in determing the heat transfer in conditions and mixtures whose flame speed and temperature have been experimentally determined.

ACKNOWLEDGEMENT

This work was carried out under the auspices of the U.S. Department of Energy at Sandia National Laboratories under contract No. DE-AC03-76SF00098 and at Lawrence Livermore National Laboratory under contract No. W-7405-ENG-48.

REFERENCES

1) Afgan, N.H. and Beer, J.M. (eds.), Heat Transfer in Flames, Scripta Book Company, New York, (1974).

2) Mondt, J.R., "Heat-Transfer Research on Internal-Combustion-Engine Systems", General Motors Ressearch Publication GMR-4147 (1982).

3) Paillard, C., Dupre, G., Combourieu, J., Fokeev, V.P., Gvozdeva, L.G. and Bazhenova, T.V., in Gasdynamics of Detonations and Explosions, Vol. 75 of Progress in Astronautics and Aeronautics, AIAA, N.Y., N.Y., pgs. 134-149 (1981).

4) Keiper, R. and Spurk, J.H., Journal of Fluid Mechanics, 113, 333-346 (1981).

5) Heperkan, H.A. and Greif, R., Int. J. Heat Mass Transfer, 25, 267-277 (1982).

6) Isshiki, N. and Nishiwaki, N., Proceedings of the Fifth International Heat Transfer Conference, II, 344-348 (1974).

7) Woodard, J.B., "An Experimental and Theoretical Study of Heat Transfer in Constant Volume and Compression-Expansion Systems Including the Effects of Flame Propagation", Ph.D. Thesis, U.C. Berkeley, March 1982.

8) Annand, W.J.D., Proceedings of the Institution of Mechanical Engineers, 177, 973-990 (1963).

9) Alkidas, A.C. and Myers, J.P., "Transient Heat-Flux Measurements in the Combustion Chamber of a Spark-Ignition Engine", ASME Report No. 81-WA/HT-1 (1981).

10) Vosen, S.R., "Unsteady Heat Transfer During the Interaction of a Laminar Flame with a Cold Wall", Ph. D. Thesis, U.C. Berkeley, December 1983.

11) Carlslaw, H.S. and Jaeger J.C., Conduction of Heat in Solids, Oxford University Press, London (1948).

12) Kays, W.M. and Crawford, M.E., Convective Heat and Mass Transfer, Second Edition, McGraw-Hill, New York (1980).

13) Andrews, G.E. and Bradley, D., Combustion and Flame, 19, 275-288 (1972).

14) Lund, C.M., HCT - A General Computer Program for Calculating Time-Dependent Phenomena Involving One-Dimensional Hydrodynamics, Transport, and Detailed Chemical Kinetics, Lawrence Livermore National Laboratory report UCRL-52504

(1978).

15) Westbrook, C.K., Adamczyk, A.A. and Lavoie, G.A., Combustion and Flame, **40**, 81-99 (1981).

16) Westbrook, C.K. and Dryer, F.L., Combustion Science and Technology, **27**, 31-43 (1981).

17) Kurkov, A.P., "A Theoretical Study of Flame Extinction by a Cold Wall and Flame Ignition by a Hot Surface", Ph.D. Thesis, University of Michigan (1967).

18) Yamazaki, S. and Ikai, S., "Study on Laminar One-Dimensional Premixed Flame with Heat Loss", translated by Kazutomo Ohtake, Transactions of The Japan Society of Mechanical Engineers, **37**, p.121 (1971).

19) Ishikawa, N., "Studies of Wall Flame Quenching and Hydrocarbon Emissions in a Model Spark Ignition Engine", Ph.D. Thesis, U. C. Berkeley (1978).

20) Ferguson, C.R. and Keck, J.C., Combustion and Flame, **28**, 197-205 (1977).

Table I
Experimental and Numerical Results

p_0 (Atmos)	ψ	t_c[a] (msec)	q_c[b] $\left[\frac{MW}{m^2}\right]$	Experimental t_q (msec)	Experimental $q_{w_{max}}$ $\left[\frac{MW}{m^2}\right]$	Experimental $\frac{t_q}{t_c}$	Experimental $\frac{q_{w_{max}}}{q_c}$	Numerical $\frac{t_q}{t_c}$	Numerical $\frac{q_{w_{max}}}{q_c}$
1.10	0.7	.416	.499	.85	.20	2.03	.40	----	----
1.12	0.8	.238	.771	.58	.28	2.41	.36	2.28	.463
1.17	0.9	.153	1.07	.24	.45	1.60	.42	----	----
1.19	1.0	.100	1.38	.20	.51	2.00	.37	2.15	.363
1.18	1.1	.095	1.43	.19	.61	2.06	.43	----	----
1.17	1.2	.119	1.21	.22	.53	1.90	.44	2.28	.385

a – From Eq.(1)

b – From Eq. (2)

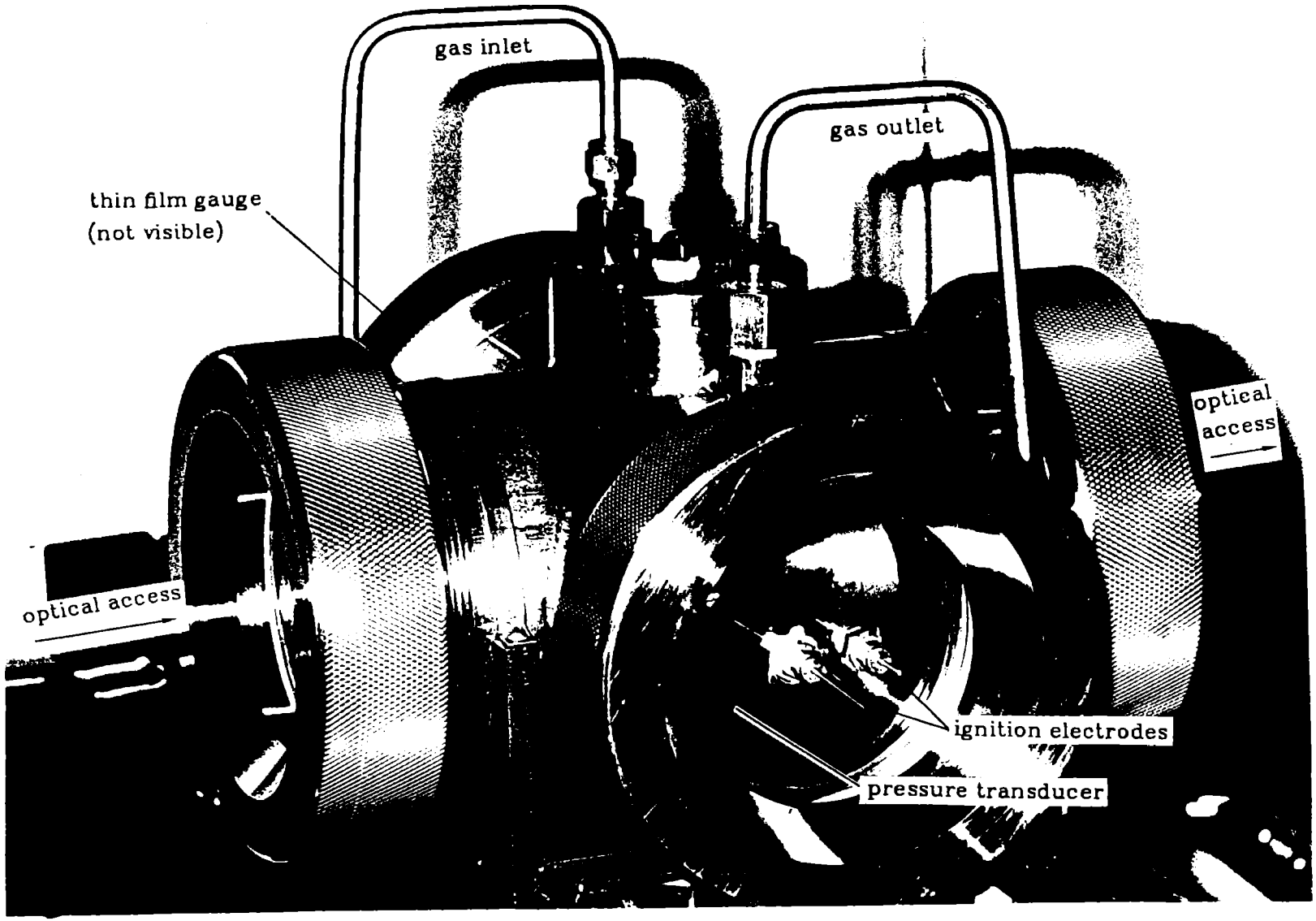

Fig. 1 Photograph of the constant volume combustion chamber.

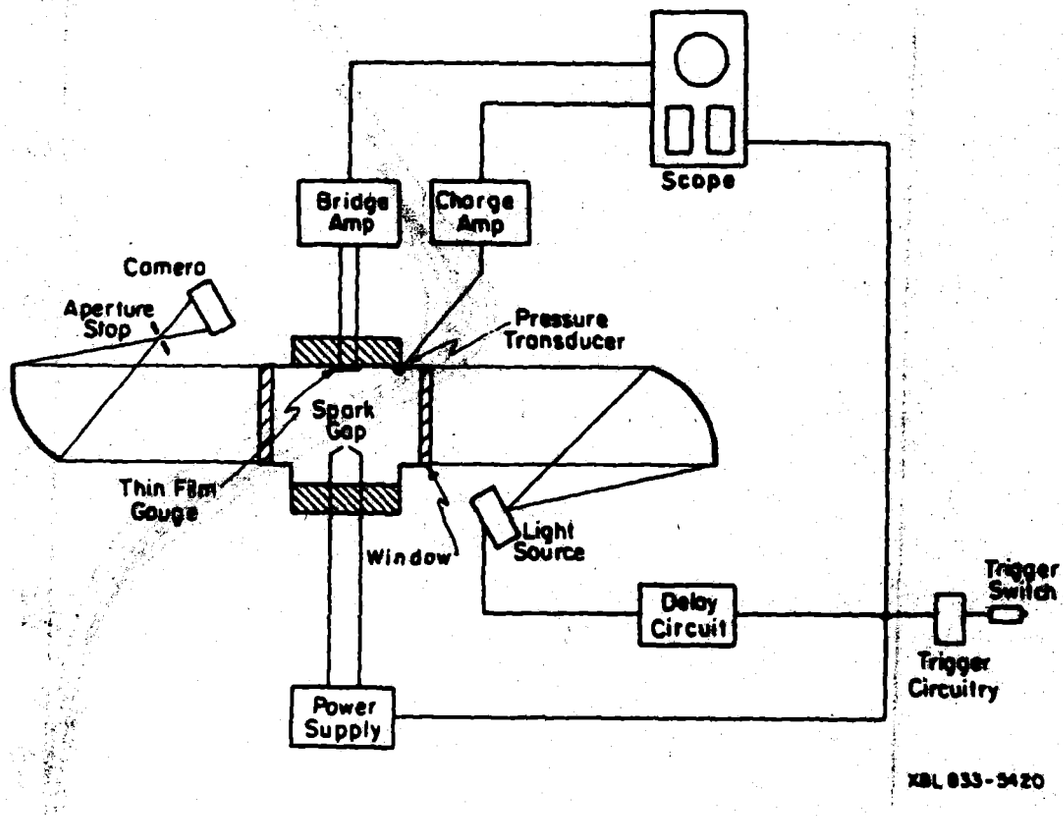

Fig. 2 Schematic of the experiment.

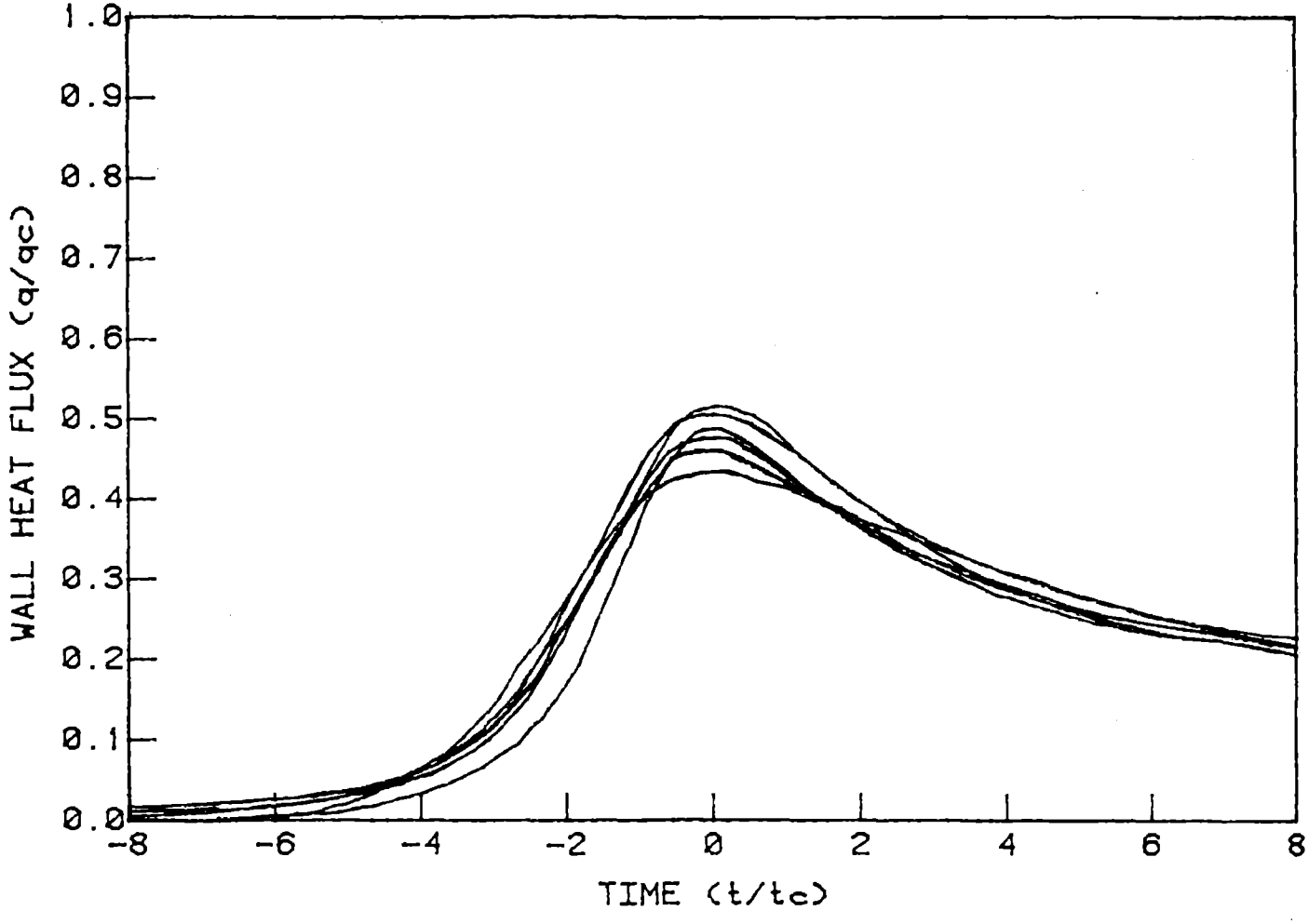

Fig. 3 Experimental results - wall heat flux vs. time.

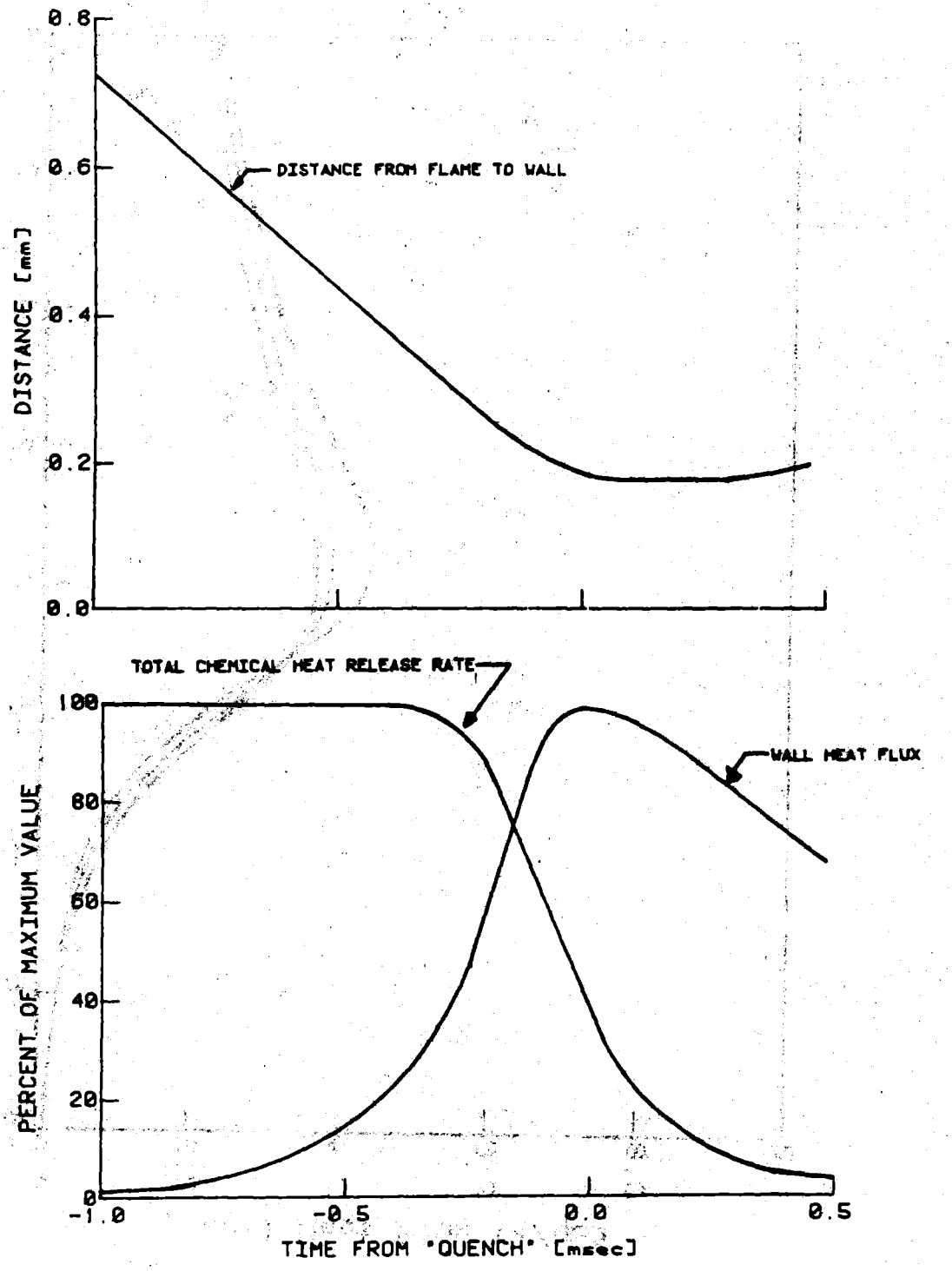

Fig. 4 Calculated heat release, wall heat flux and flame position.

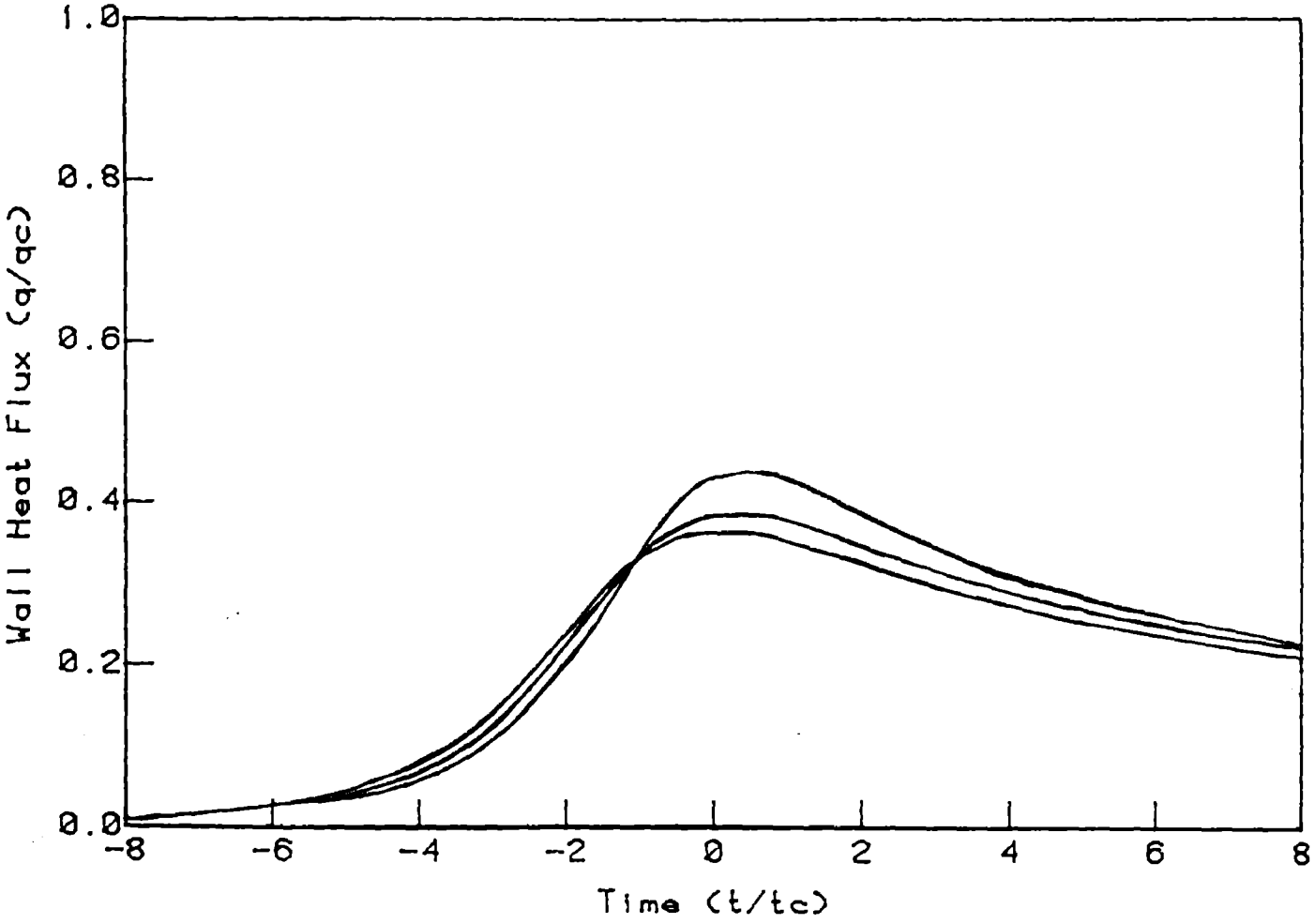

Fig. 5 Numerical results, single step kinetics - wall heat flux vs. time.

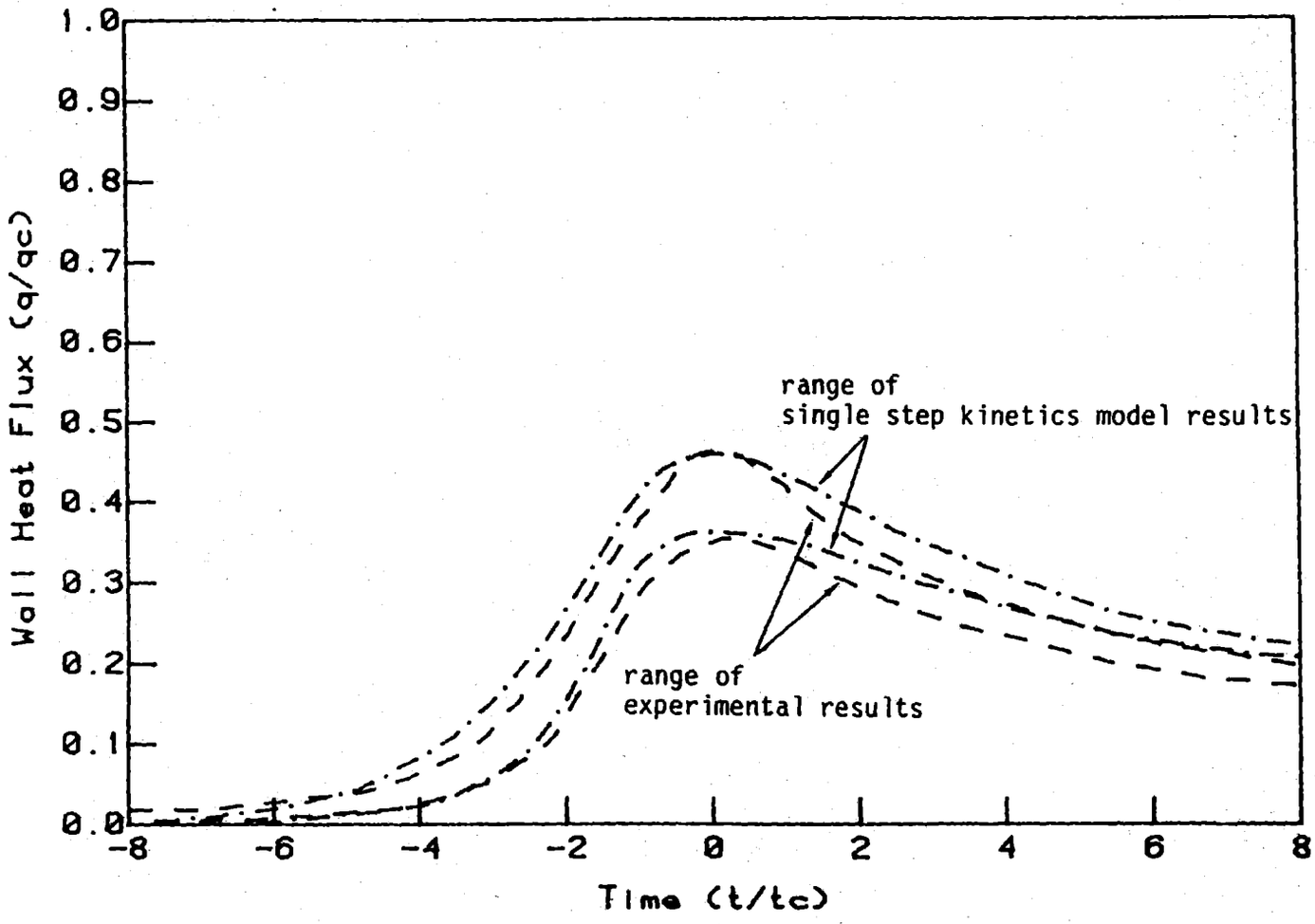

Fig. 6 Comparison of experimental results and single step kinetics model - wall heat flux vs. time.